Histopathology of *Xanthomonas campestris* pv. *citri* from Florida and Mexico in Wound-Inoculated Detached Leaves of *Citrus aurantifolia*: Transmission Electron Microscopy

M. M. Dienelt and R. H. Lawson

United States Department of Agriculture, Agricultural Research Service, Florist and Nursery Crops Laboratory, Beltsville, MD 20705.
Accepted for publication 26 September 1988 (submitted for electronic processing).

ABSTRACT

Dienelt, M. M., and Lawson, R. H. 1989. Histopathology of *Xanthomonas campestris* pv. *citri* from Florida and Mexico in wound-inoculated detached leaves of *Citrus aurantifolia*: transmission electron microscopy. Phytopathology 79:336-348.

Detached leaves of *Citrus aurantifolia* were wound-inoculated with pathogens *Xanthomonas campestris* pv. *citri* XC90, a Mexican strain inducing raised blisters; *X. c. citri* F1, a Florida strain inducing water-soaking; *X. c. citri* F20, a Florida strain inducing small necrotic lesions; non-citrus pathogen *X. c. pruni* XP1; saprophyte *Erwinia herbicola* EH1; or water. Cytological changes were traced from the wound to bacterial localization and were divided into six zones. In water, XP1 and EH1 inoculations, the wound is bordered by disrupted cells (zone one), followed by modified preexisting cells similar to impervious tissue (zone two) and a periderm (zone three). Zone two modifications include suberin wax lamellae on inner cell walls, outer wall surface lamellae, wall projections, thick layered cell walls, and intercellular accumulations of osmophilic granules. Zones one through three develop abnormally and are followed by regions of bacterial invasion (zone four) and localization (zones five and six) in leaves wound-inoculated with strains of *X. c. citri*. Zones five and six resemble wound repair zones two and three, respectively, with zone five osmophilic granule production followed by zone six host cell division. When surrounded by osmophilic granules at the wound, bacteria of all strains are immobilized; however, localization of *X. c. citri* is incomplete until zone five. The three isolates of *X. c. citri* can be distinguished in zones one through four. Strain XC90 stimulates, but strain F1 suppresses osmophilic granule production, wall modifications, and cell division at the wound. In zone four, strains F1 and F20 are present primarily in intercellular spaces, but strain XC90 invades along middle lamellae of proliferating cells. Both Florida strains are associated with a fibrillar matrix that does not occur in XC90 infections. Wound repair abnormalities, patterns of invasion, and the fibrillar matrix provide the major cytological points of strain differentiation.

Xanthomonas campestris pv. *citri* (Hasse) Dye, which causes citrus bacterial canker disease, typically induces a raised pustule symptom. Strains of *X. c. citri* have been isolated in Florida that cause symptoms ranging from slight necrotic flecking to expanding water-soaked lesions. Based on symptomatology, host range, geographical distribution, and genomic fingerprints, these strains have been placed into a separate group (group E) to distinguish them from strains in groups A, B, C, and D (7,16).

Histological comparisons between two Florida strains and a Mexican strain of *X. c. citri* revealed that the Mexican strain stimulated host cell division in wound repair tissues while the Florida isolates suppressed it, either significantly in the case of an aggressive strain or slightly in the case of a nonaggressive strain (24). The Florida strains were also associated with an intercellular matrix that was not present in infections caused by the Mexican isolate.

Because comparisons between the Mexican and Florida strains used a wound-inoculation system, a zone system was established that, while based on wound-induced host modifications, could also be used in infected tissue where wound-repair was altered. In water controls, zone one is adjacent to the wound and contains disrupted cells, zone two is composed of preexisting cells with thick cell walls and occluded intercellular spaces, and zone three is a periderm. Infection by *X. c. citri* causes strain specific alterations in each zone (24).

In this report, comparisons between the Florida and Mexican isolates are described at the ultrastructural level. Zonal notation is expanded to include zones four, five, and six, with zones five and six representing zones of pathogenic bacterial localization and zone four representing the tissue between wound repair and localization.

MATERIALS AND METHODS

Bacterial cultures. Bacterial cultures included three pathogenic strains of *X. c. citri*, saprophytic *Erwinia herbicola* (Lohnis) Dye EH1, and a non-citrus pathogen, *X. c. pruni* (Smith) Dye XP1. Strain XC90 of *X. c. citri* was isolated from raised lesions on *Citrus aurantifolia* Swingle in Mexico, strain F1 from a flat, expanding, water-soaked leaf lesion on Carrizo citrange (*Poncirus* Raf. × *C. sinensis* Osbeck) in Florida, and strain F20 from a flat, nonexpanding necrotic leaf lesion in grapefruit, *C. paradisi* Macfady, in Florida.

Inoculation and incubation. Detached leaves of *C. aurantifolia* were inoculated and incubated as previously described (24). Sterile distilled water or bacterial suspensions containing 1×10^7 cells per milliliter were placed as 10-μl drops on each of 10–12 fresh punctures per leaf. Leaves were placed on 1% water agar, and petri dishes were sealed and incubated under controlled environmental conditions (24).

Sampling and processing. Leaf pieces about 2 mm square were removed around centrally located wound sites, containing green symptomless tissue when possible. Samples were taken 1, 2, 3, 4, 5, 7, 10, and 14 days after inoculation in at least three separate experiments. Seven-day samples included nonwounded controls. Tissue was fixed at 4 C in 2% glutaraldehyde and 1.5% acrolein in 0.05 M Na_2HPO_4-KH_2PO_4(PO_4), pH 7.0. Samples were postfixed in 1% OsO_4, dehydrated in ethyl alcohol, and embedded in Spurrs' epoxy resin. Ultrathin sections were stained 45 min with uranyl acetate and 15 min with Reynolds lead citrate.

RESULTS

Healthy wound repair. *Zone one.* Twenty-four hours after wounding, contents of punctured and adjacent cells were disrupted and dispersed. Outer cell wall surfaces (bordering intercellular spaces) appeared frayed and sparsely lined with electron-dense amorphous and fibrous/particulate substances. By 48 hr, osmophilic granules were associated with outer walls and electron-dense particulate lined surfaces normally adjacent to plasmalemmae (inner walls) (Fig. 1A and B). Concentrations of osmophilic granules towards the edge of zone one increased within cells, on outer cell wall surfaces, and in intercellular spaces with increased time from wounding.

Zone two. Preexisting cells at the inner edge of zone one

contained peripheral cytoplasm, rather than the dispersed cytoplasmic remnants and osmophilic granules that filled lumens of zone one cells. While zone two cytoplasm appeared intact in early wound repair (Fig. 1C), it gradually condensed to electron-dense peripheral strands. Inner cell walls showed a striated banding pattern typical of suberin wax lamellae (6,10,28) formed in phellem cells (see zone three).

Extensive deposition of granular and opaque electron-dense material occurred on or in middle lamellae, cell walls, and intercellular spaces (Figs. 1C and 2A–C). Osmophilic granules were more numerous and heterogeneous in zone two than in zone one. Granules appeared in intercellular spaces (Figs. 1C and 2A, C), lining cell walls (Fig. 2A), concentrated at junctions formed by middle lamellae and outer walls of adjoining cells (Fig. 1C) and within granular outer wall appositions (Fig. 2C). Electron-dense pellicles often bordered granular accumulations (Fig. 1C). Granules closest to cell walls were larger and more electron-dense than those more distant in the intercellular space (Fig. 2A).

Cell walls became thick and often developed a layered appearance (Fig. 2C). In addition to granular appositions, outer

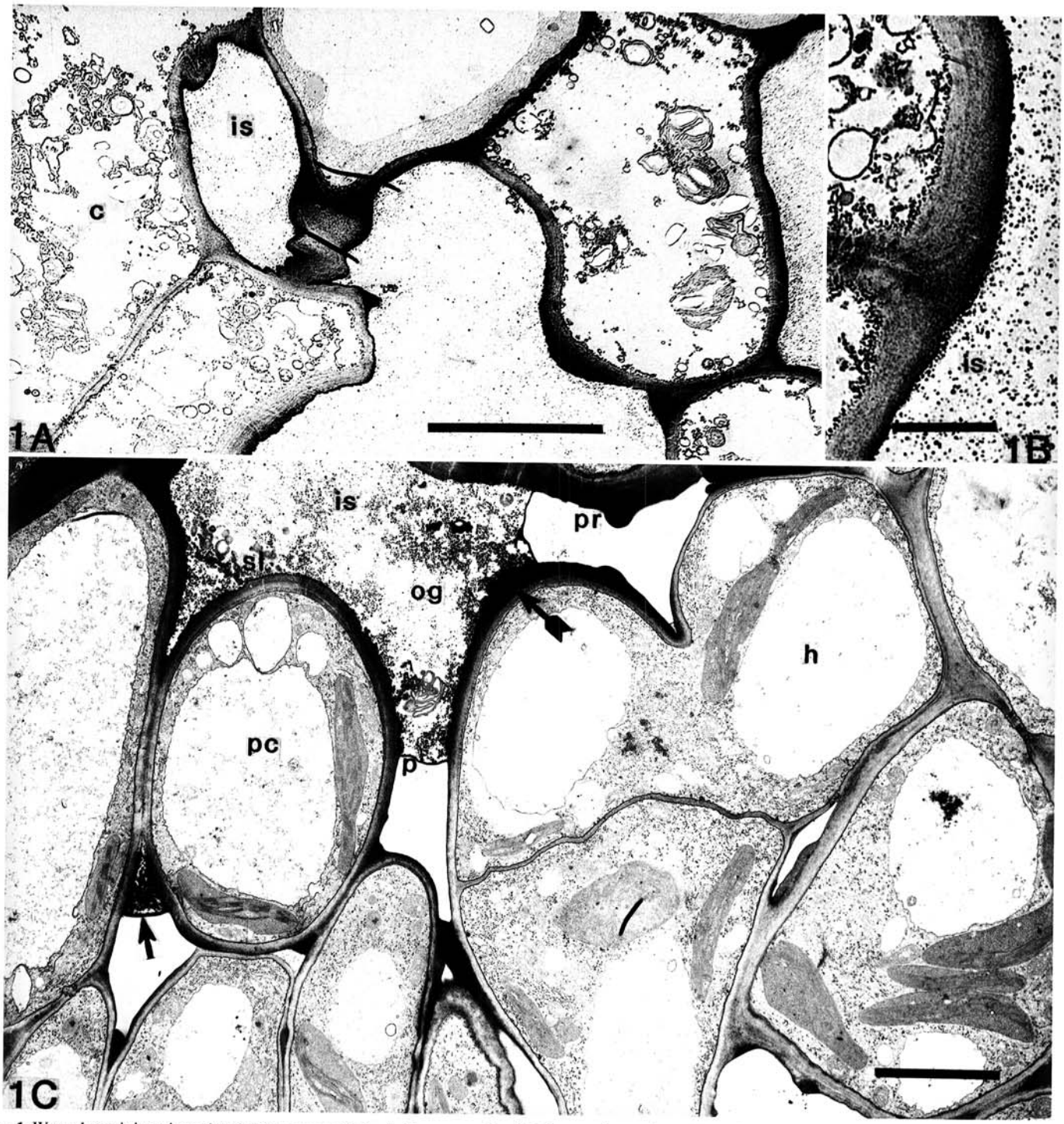

Fig. 1. Wound repair in uninoculated *Citrus aurantifolia*. **A,** Zone one cells with disrupted cytoplasm (c) and intercellular spaces (is) containing osmophilic granules. Tissue was harvested 2 days after inoculation, and the wound is to the left. Bar = 10 μm. **B,** Higher magnification of zone one osmophilic granules in intercellular spaces (is), 2 days after inoculation. Bar = 2 μm. **C,** Zone two preexisting cells (pc) and zone three hyperplasia (h), indicating periderm initiation at 3 days. Modifications include: osmophilic granules (og) bordered by pellicles (p) in intercellular spaces (is) or over middle lamellae (arrowhead), cell wall projections (pr), surface lamellae (sl) developing on outer wall surfaces, and increased electron density (arrow) in cell walls and middle lamellae. The wound is to the left. Bar = 5 μm.

walls and middle lamella junctions developed surface lamellae (Figs. 1C and 2A) and opaque projections (Fig. 1C). Surface lamellae initially appeared as narrow pellicles that became globular and thicker as wound repair progressed, apparently through aggregation of osmophilic granules (Fig. 2A).

As cell walls became thicker and osmophilic granules became more concentrated, the area corresponding to zone two often crumbled during sectioning. By 10 days, zone two frequently appeared full of holes.

Zone three. Between 24 and 48 hr, hypertrophy developed in some preexisting cells (Fig. 2B), frequently in bundle sheath or vascular parenchyma cells. Electron-dense accumulations plugged intercellular spaces and enclosed junctions formed by middle lamellae and outer walls of adjoining cells. By 72 hr, hypertrophic cells had divided, and a periderm was discernible at the inner edge of zone two between 4 and 5 days (Fig. 2C).

Phellem cells and zone two cells displayed many similar characteristics including: Cell wall thickening, formation of outer wall appositions and surface lamellae on phellem wall surfaces bordering zone two, striated bands on inner walls (Fig. 2D), and electron-dense, peripheral cytoplasm. Osmophilic granules often permeated intercellular spaces between phellem and zone two.

Newly formed periderm cell walls remained thin, with outer wall thickening restricted to original hyperplastic cells and thickened, star-shaped areas representing junctions of coalescing newly formed middle lamellae. The latter contained electron-dense opaque or fibrous material.

Nonwounded tissue. Cell walls of nonwounded tissue appeared moderately and evenly stained with smooth outer wall surfaces. The electron-dense cell walls, outer wall surface lamellae, granular wall appositions, and irregular projections characteristic of zone two and phellem cell walls were not observed. Osmophilic granules did not develop, and intercellular spaces remained electron-lucent.

Strain F20. *Zone one.* Host cell walls closest to the wound appeared bleached, swollen, and separated compared with walls of zone one cells in normal wound repair (Fig. 3A). Only a few bacteria were present at 48 hr and were predominantly intercellular. Higher populations were present at 72 hr. By 10 days, most organisms had degenerated.

Zone two. Cytoplasm in many preexisting cells condensed as in

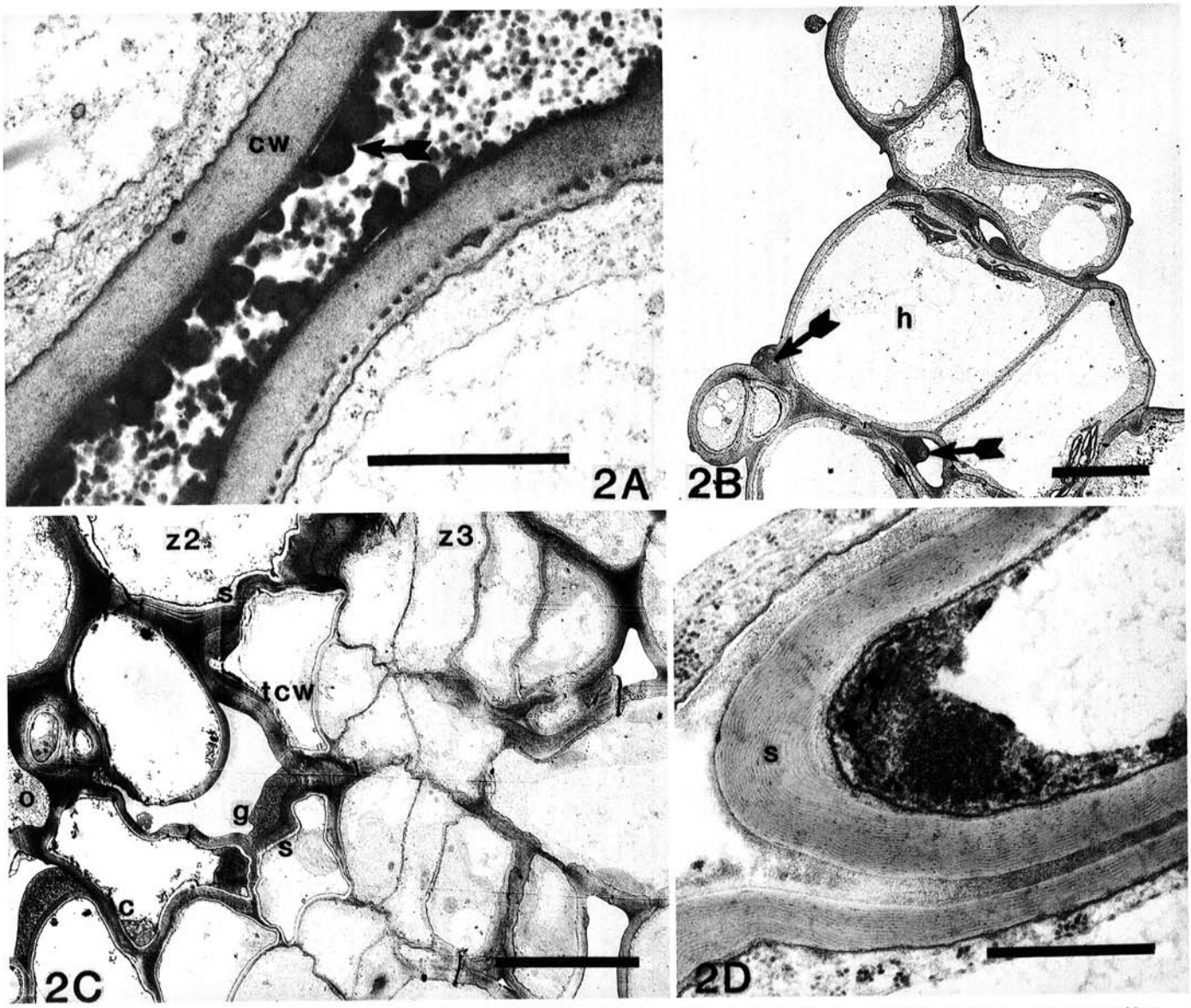

Fig. 2. Wound repair in uninoculated *Citrus aurantifolia*. **A,** Zone two, 3 days after inoculation. Small and large osmophilic granules are present, and larger granules are aggregating (arrow) as part of early surface lamella formation on outer cell walls (cw). Bar = 1 μm. **B,** Periderm initiation in zone three at 2 days after inoculation. Hyperplasia (h) is evident and electron-dense substances (arrows) have accumulated over middle lamella junctions and within intercellular spaces. The wound is to the left. Bar = 10 μm. **C,** Mature zones two (z2) and three (z3), 5 days after inoculation. Modifications include: suberin/wax lamellae (s) on inner cell walls, thick layered walls (tcw), granular wall appositions (g), constricted cytoplasm (c) in zone two and phellem cells, intercellular space occlusion (o) with osmophilic granules, and increased electron density in cell walls and middle lamellae. The wound is to the left. Bar = 10 μm. **D,** Phellem, 10 days after inoculation. The suberin/wax lamella (s) contains characteristic striations. Bar = 0.5 μm.

healthy wound repair zone two cells. Suberized cells with a striated banding were observed only in cells closest to the periderm. Integrity of thickened walls appeared disrupted as outer surfaces protruded into intercellular spaces and granules were observed within wall structure (Fig. 3B). Many walls appeared thin and distorted.

Zone three. Periderm initiation appeared similar to that in water-inoculated controls. By 5 days, periderm formation was often incomplete, with intercellular spaces present. Regular rows of congruent isodiametric cells did not always develop (Fig. 3B).

At 72 hr, bacteria were present intercellularly at the walls of immature phellem cells (Fig. 3C). Fibers appeared along cell wall surfaces and the resulting open structure revealed osmophilic granules deep within thickening walls (Fig. 4A). Despite an initial open structure, by 7 days surface lamellae were fully formed, and phellem cell walls appeared intact, electron dense, and thickened (Fig. 4B).

By 10 days, dense accumulations of intercellular granules were present between zone two and phellem cells. Pellicle-bound granules over middle lamella junctions and bridging neighboring cells often contained degenerating bacteria (Fig. 4B). Many bacteria were not confined, however, and large numbers of organisms were observed beyond the phellem.

Bacterial movement through the periderm appeared to be both inter- and intracellular (Fig. 4C), although intercellular organisms often appeared to be immobilized by osmophilic granules. Intracellular invasion was preceded by degeneration of outer walls and accumulation of electron-dense material between inner walls and the plasmalemma. Numerous cytoplasmic vacuoles developed. After plasmalemma destruction, inner walls

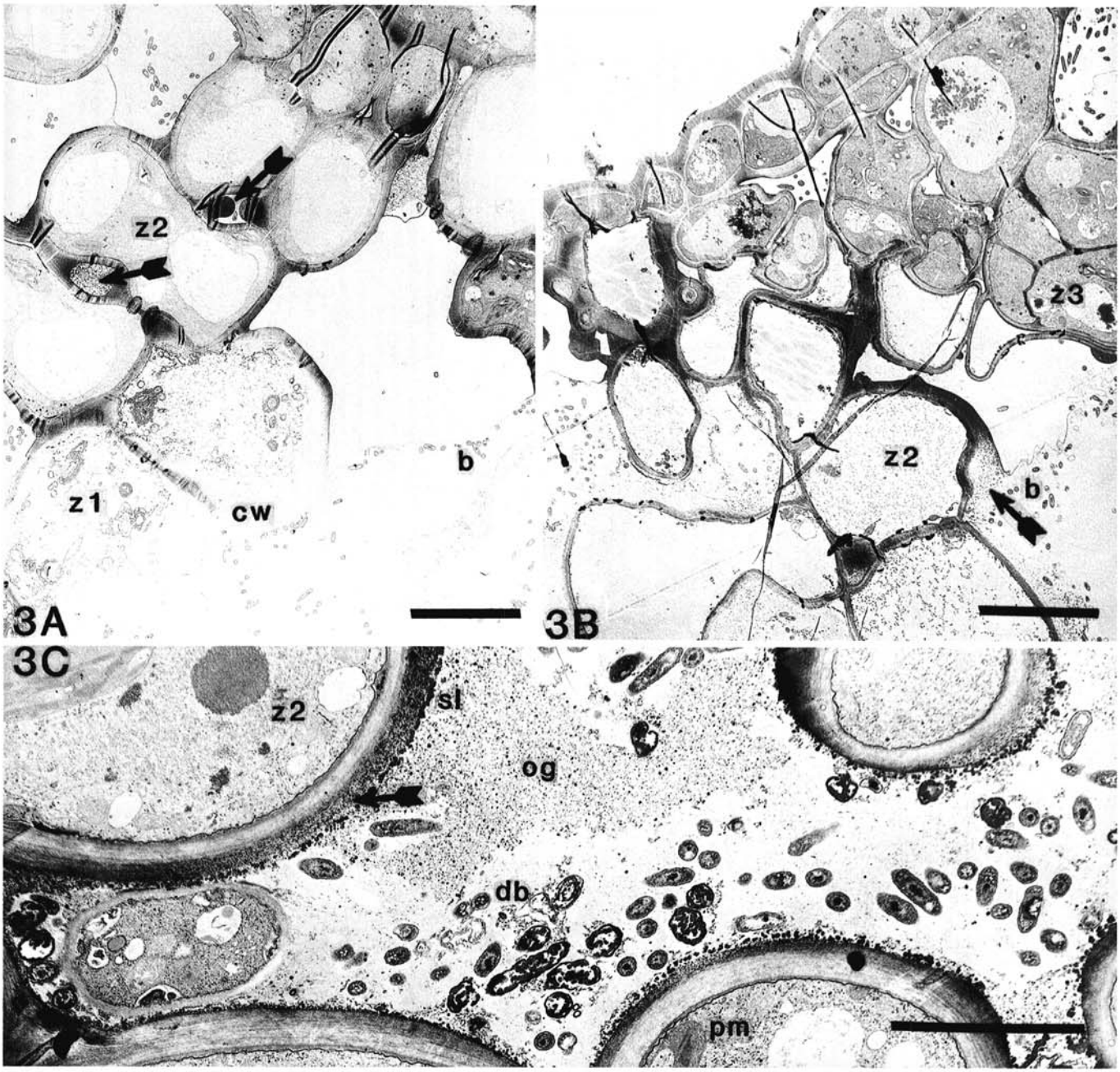

Fig. 3. Interactions between strain F20 of *Xanthomonas campestris* pv. *citri* and wound repair in *Citrus aurantifolia*. **A,** Bacteria (b) and zones one (z1) and two (z2), 3 days after inoculation. Cells in zone one have faint, separating walls (cw). Intercellular space occlusions (arrows) are present in zone two. The wound is to the right. Bar = 10 μm. **B,** Bacteria (b) and zones two (z2) and three (z3), 10 days after inoculation. Cell wall thickening is disrupted in zone two (arrow), and zone three periderm is not resolved into regular rows of isodiametric cells. The wound is to the left. Bar = 10 μm. **C,** Zone two (z2) and phellem (pm), 3 days after inoculation. Granules are present in thickening cell walls (arrow). Surface lamellae (sl) have formed, and intercellular osmophilic granules (og) and degenerating bacteria (db) are apparent. Bar = 5 μm.

degenerated, releasing fibers and particulate materials into cell lumens. Cells were subsequently colonized or collapsed. Bacteria were surrounded by a fibrous matrix (Fig. 5A).

Zone four. Bacterial invasion beyond the periderm occurred both inter- and intracellularly (Fig. 5A). Intracellular invasion patterns were similar to those in zone three; however, intercellular immobilization did not occur. Bacteria appeared intact, cell walls did not display thickening, and osmophilic granules were not observed.

Zone five. At the inner edge of zone four, osmophilic granules began accumulating on outer cell wall surfaces and bacteria within granules degenerated (Fig. 5A and B). Nearby fibrous matrix became increasingly electron dense, and associated bacteria were immobilized (Fig. 5A). With increased electron-dense

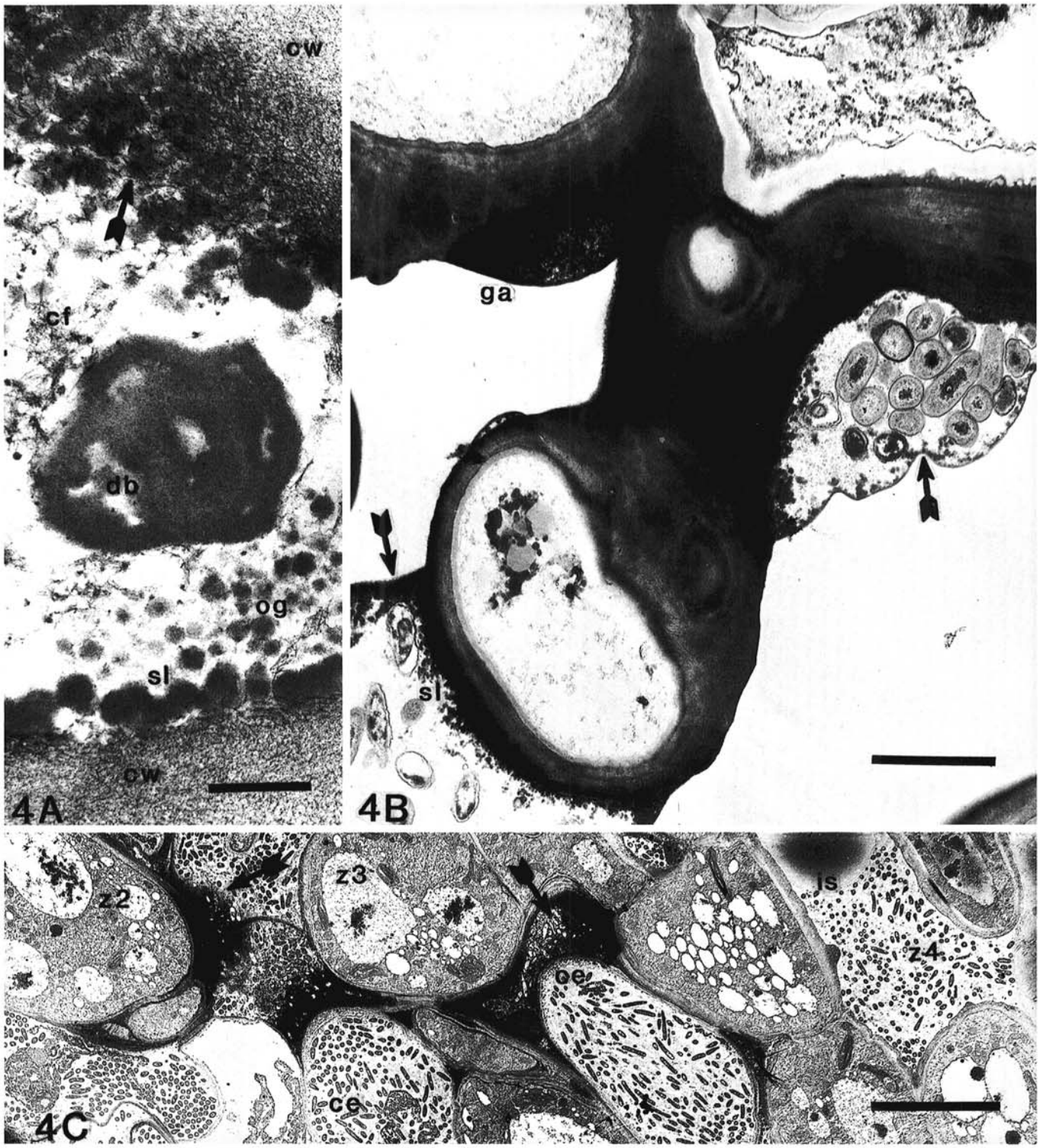

Fig. 4. Interactions between strain F20 of *Xanthomonas campestris* pv. *citri* and wound repair in *Citrus aurantifolia*. **A,** High magnification of phellem cell walls (cw) showing osmophilic granules within walls with loosened fibers (arrow) and the formation of surface lamellae (sl). A degenerating bacterium (db) is near intercellular granules (og) and liberated wall fibers (cf), 3 days after inoculation. Bar = 250 nm. **B,** Cell wall recovery in zone two and phellem at 7 days after inoculation. Cell walls are thick and intact, granular apposition (ga) and surface lamellae (sl) are present, and bacteria are immobilized within pellicle-bound accumulations of granules (arrow). Bar = 2 μm. **C,** Bacterial invasion of zones two (z2), three (z3), and four (z4). Bacteria are immobilized in osmophilic substances of zone two and three intercellular spaces (arrows), but not within colonized zone three cells (ce) or zone four intercellular spaces (is). Ten days after inoculation. The wound is to the left. Bar = 10 μm.

accumulations in intercellular spaces and on host outer wall surfaces, host wall damage and intracellular invasion decreased. Toward the edge of invasion, deposits acquired a stratified appearance. Accumulations adjacent to outer cell walls appeared opaque and wall-like (Fig. 5C), but those toward the center of intercellular spaces appeared granular (Fig. 5B). Bacteria were degenerating and confined within osmophilic deposits.

Zone six. Hyperplastic cells studded with irregular wall projections developed at the edge of invasion, appearing similar to hyperplastic cells, and appositions formed during early wound repair. Intercellular spaces between hyperplastic cells were occluded with osmophilic granules.

Strain F1. *Zone one.* Host cell walls lacked linings of osmophilic substances and appeared swollen and diffuse (Fig. 6A). Intercellular spaces often contained large patches of loose fibers. Outer walls and middle lamellae became increasingly electron dense, and by 2 wk, appeared as electron-dense, ribbonlike structures.

Bacteria were present in high numbers both inter- and intracellularly within 24 hr after inoculation. Organisms were typically clustered at cell walls, appearing in cells as wall fibers dispersed. By 2 wk, bacteria were reduced in number or absent.

Zone two. In preexisting cells abutting zone one, cytoplasm became increasingly electron-lucent, plasmalemmae disappeared, and inner walls were swollen and diffuse, appearing similar to zone one cells. Suberin wax bands and thickened walls with granular appositions, opaque projections, and surface lamellae did not develop. Osmophilic granules were not observed except as sparse accumulations in epidermal cells. By 7 days, cellular content was reduced to faintly stained vesicles and cell wall fibers. As in zone one, cell walls were increasingly thin and electron dense at outer walls and middle lamellae.

Zone three. Cells became hypertrophic by 48 hr; however, cell division ceased after 4 days, and a periderm did not develop. Instead, zone three was composed of separated hyperplastic cells having undergone one to three divisions. Cell walls often displayed a characteristic double-walled appearance (Fig. 6C).

At 4 days, bacteria were observed between hyperplastic cell walls (Fig. 6D). Outer wall surfaces appeared frayed, uneven, and lined with nearby patches of wall fibers. Plasmalemmae were convoluted and associated with depositions of electron-dense material. Endoplasmic reticulum appeared prominent and swollen, often forming a spiral pattern (Fig. 6B) that was observed in cells throughout the lesion. By 7 days, high concentrations of organisms and a fibrillar matrix at middle lamellae had pushed cell walls apart, resulting in extensive host wall folding (Fig. 6E). Remaining

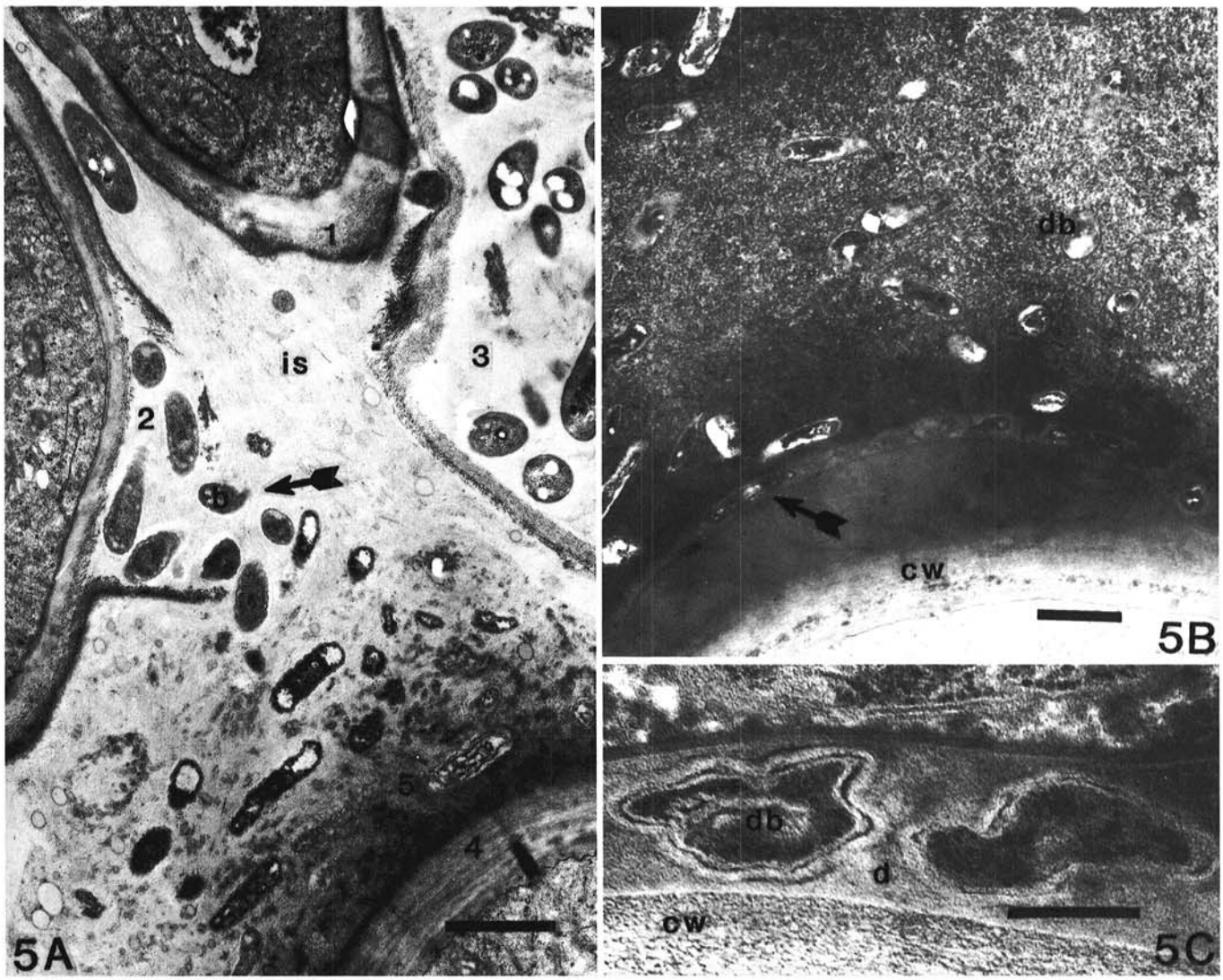

Fig. 5. Localization of strain F20 of *Xanthomonas campestris* pv. *citri* beyond wound repair in *Citrus aurantifolia*. **A,** Zone four/five transition, 10 days after inoculation. Four cells show initial loosening of wall fibers (1), more advanced wall dissolution (2), intracellular invasion (3), and an intact wall (4) associated with the presence of immobilizing osmophilic substances (5). A fibrillar matrix (arrow) surrounds bacteria (b) in intercellular space (is). Bar = 1 μm. **B,** Edge of invasion, zone five, at 10 days after inoculation. Bacteria (db) are immobilized in osmophilic substances, including granules and dense wall-like depositions (arrow) on outer wall (cw) surfaces. Bar = 1 μm. **C,** High magnification of bacteria (db) immobilized in wall-like deposition (d) abutting a host cell wall (cw). Bar = 250 nm.

cell walls and middle lamellae became increasingly electron dense, and additional host wall degradation was not observed. By 2 wk, although empty hypertrophic cells were still discernible, many cells had collapsed.

Zone four. Bacteria were present beyond regions of potential wound repair zones within 2 days after inoculation, before the first

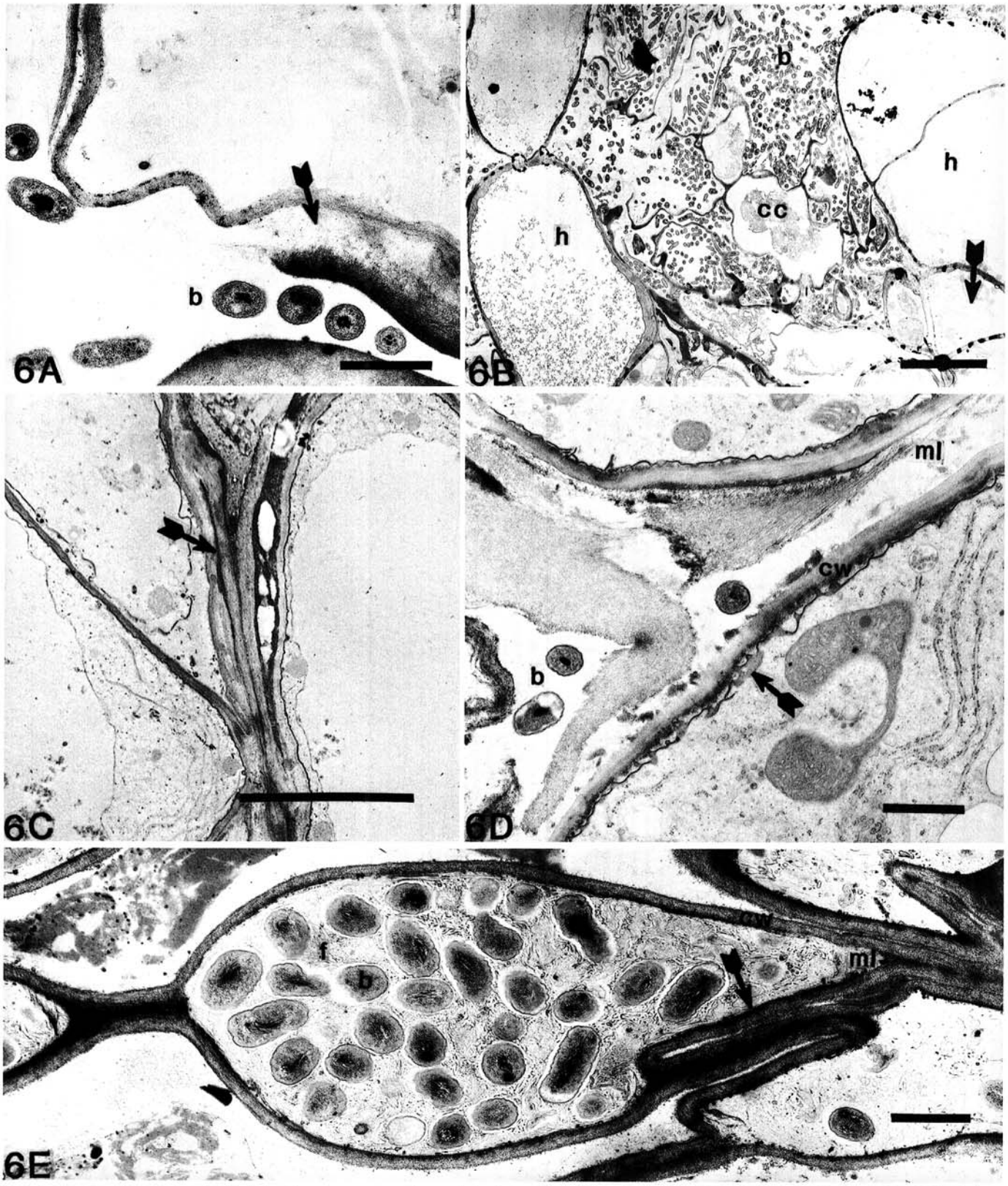

Fig. 6. Interactions between strain F1 of *Xanthomonas campestris pv. citri* and wound repair in *Citrus aurantifolia*. **A,** Bacteria (b), host cell wall dissolution (arrow), and absence of osmophilic granules characterize zone one, 2 days after inoculation. Bar = 1 μm. **B,** Region of cell collapse (cc) and hyperplasia (h) corresponding to zones two and three and distinguished by high bacterial (b) numbers and the absence of wall modifications, osmophilic granules, and cambium formation. Endoplasmic reticulum (arrow) may be prominent. The wound is toward the upper left. Bar = 10 μm. **C,** Double-walled (arrow) appearance of hyperplastic cells, 5 days after inoculation. Bar = 5 μm. **D,** Zone three, 10 days after inoculation. Bacteria (b), dissolving hyperplastic cell walls (cw) and middle lamellae (ml), and opaque accumulations (arrow) at the plasmalemma are present. Bar = 1 μm. **E,** High concentrations of bacteria (b) and associated fibrillar matrix (f) at the middle lamella (ml) with extensive cell wall (cw) separation and folding (arrow), 14 days after inoculation. Bar = 1 μm.

wound-induced host cell division had occurred. Organisms were observed in mesophyll intercellular spaces (Fig. 7A), xylem vessels, substomatal cavities, stomatal openings, and on nearby epidermal surfaces. Bundle sheath cells often became hyperplastic.

Intercellular spaces contained large numbers of organisms, fibrillar matrix, and fibrous/particulate accumulations (Fig. 7B). Fibrillar matrix typically surrounded bacteria and often included small moderately stained vesicles (Fig. 7C). Fibrous/particulate accumulations rarely contained bacteria and appeared associated with the host (Fig. 7B). By 7 days, layers of short electron-dense fibers and/or an amorphous electron-dense material had developed on outer cell walls (Fig. 7C).

In some cells, cytoplasm appeared grainy and electron dense, with distorted tonoplasts, numerous mitochondria, small vacuoles with faintly stained content, and reduced chloroplast membranes present (Fig. 7D). Swollen ER similar to that observed in zone three was prevalent. As degeneration advanced, cytoplasm assumed a grainy particulate appearance indistinguishable from the grainy particulate matter filling central vacuoles. Such cells corresponded to blue cells observed by light microscopy (24). By 10–14 days, many cells were empty, but cell walls remained intact.

Zone five. Between 5 and 7 days, extensive concentrations of osmophilic granules began filling intercellular spaces and substomatal cavities. Bacterial cell walls appeared coated with granules (Fig. 7E). Host cell wall fibers, nearby host-associated fibrous/particulate, and bacteria-associated fibrillar matrix became increasingly electron dense (Fig. 8A). Bacterial cell walls appeared thick, electron dense, and frequently vesiculating, adding to osmophilic accumulations.

Zone six. Bacterial invasion often extended beyond the edge of the sample; however, in some 7–14-day infections, invasion was stopped by immobilization of bacteria within osmophilic accumulations lining intercellular spaces (Fig. 8B). Nearby cells became hypertrophic and contained irregular wall projections similar to those observed in developing periderms of water-inoculated controls and in zone six of F20 infections.

Strain XC90. *Zone one.* Host cells appeared similar to water-inoculated controls for 3–5 days (Fig. 9A). Only a few bacteria were present. Host walls degenerated and, by 2 wk, zone one was composed of thin-walled collapsed cells, ribbons of electron-dense

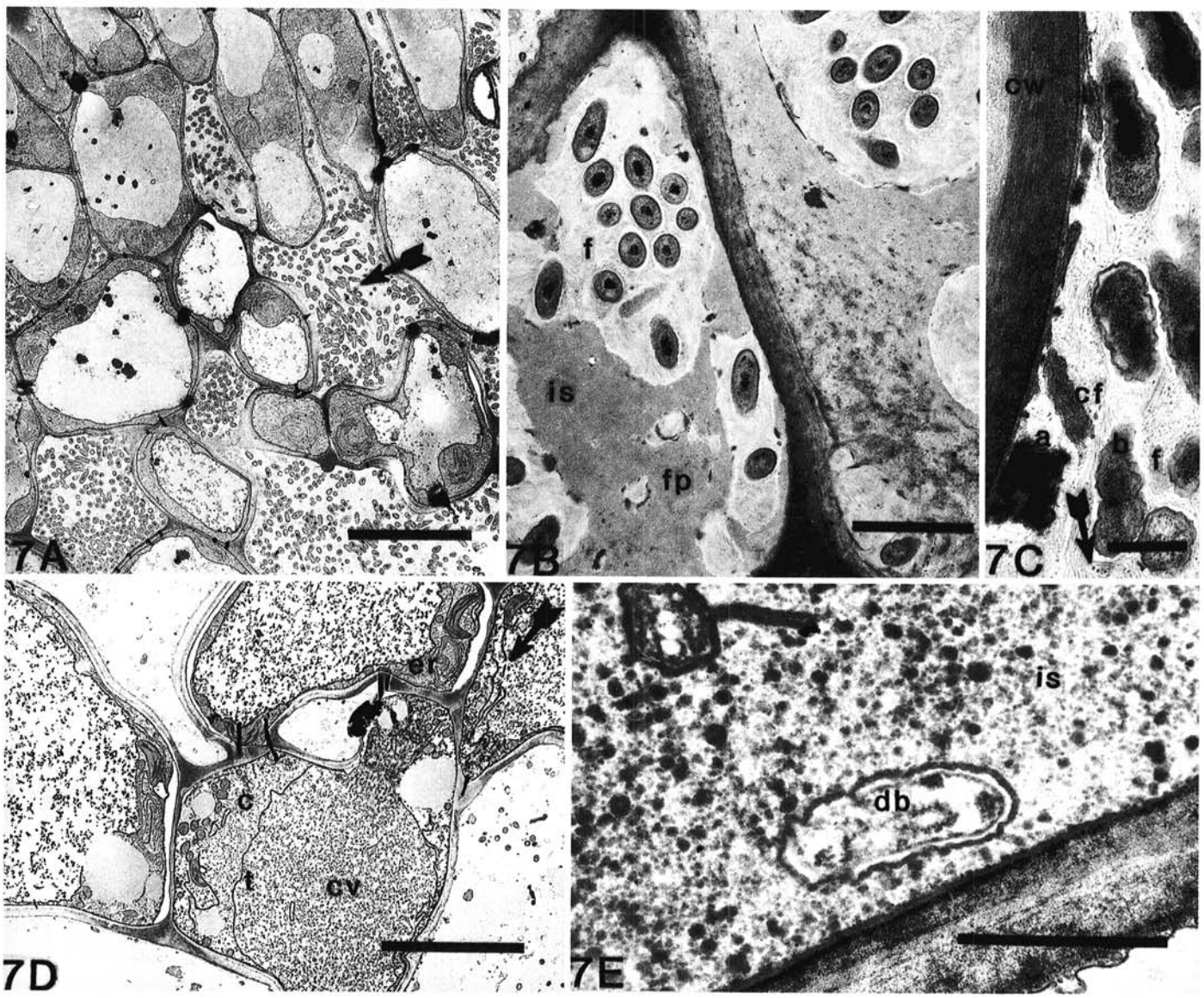

Fig. 7. Invasion and localization of strain F1 of *Xanthomonas campestris* pv. *citri* beyond the wound in *Citrus aurantifolia*. **A,** High numbers of intercellular bacteria (arrow) in zone four, 7 days after inoculation. Bar = 10 μm. **B,** Bacteria-associated fibrillar matrix (f) and host-associated fibrous particulate material (fp) in zone four intercellular spaces (is), 4 days after inoculation. Bar = 2 μm. **C,** Fibers (cf) and amorphous material (a) released from host cell walls (cw) in zone four. Bacteria (b) are surrounded by fibrillar matrix (f) and vesicles (arrow), 10 days after inoculation. Bar = 0.5 μm. **D,** Zone four, 10 days after inoculation. Degenerating cells are distinguished by cytoplasmic (c) dissolution, central vacuoles (cv) with particulate content, tonoplast (t) distortion, and breakage (arrow) and prominent spiral ER (er). Bar = 10 μm. **E,** Zone five, 10 days after inoculation. Degenerating bacteria (db) are within osmophilic granules in intercellular space (is). Bar = 1 μm.

cytoplasm, high populations of bacteria, and dispersed osmophilic granules.

Zone two. Cell wall thickening, suberin lamellae, constricted cytoplasm, granular appositions, and protrusions on outer walls appeared similar to those in healthy wound repair in some samples, but in others, zone two appeared incomplete or absent (Fig. 9A). In such cases, cytoplasm appeared disperse like that in zone one cells, rather than constricting to peripheral strands. With increased time from wounding, dense accumulations of intracellular osmophilic granules developed. Fragments of wall projections and outer wall layers were often detached from the remainder of the wall. In all samples, intercellular osmophilic granule production was extensive by 5–7 days after inoculation and continued to increase, with cell walls unevenly coated with thickened surface lamellae and electron-dense substances (Fig. 9B). Associated bacteria were degenerating (Fig. 9C). By 2 wk, zone two was composed of high concentrations of granules, immobilized bacteria, and degenerating host cells.

Zone three. Periderm was distinguishable between 3 and 4 days. Striated inner wall bands in phellem cells were often narrow and incomplete. Thickening of hypertrophic cell walls was present in some cases and absent in others. Intact bacteria were observed along phellem middle lamellae, but nearby organisms in zone two intercellular spaces were degenerating in osmophilic granules (Fig. 9A). At 4 days, colonized middle lamellae contained moderately stained compact fibers (Fig. 9D), becoming increasingly less electron dense and compact by 5–7 days after inoculation. With additional dissolution, inner walls appeared thin and uneven (Fig. 9E), often degrading until only plasmalemmae remained. Phellogen was visible by 2 or 3 days after inoculation, but continued random division obscured the cambium within 7 days.

Zone four. Intracellular invasion was observed only in xylem vessels (Fig. 10A). Extensive hyperplasia precluded the development of intercellular spaces and bacteria were typically located along the middle lamella, where degradation patterns were similar to those in zone three (Fig. 10B).

Zone five. Extensive inter- and intracellular granulation of cell walls developed by 7 days, with highest concentrations located close to lower epidermal surfaces, bordering epidermal ruptures and at the far edge of cell proliferation (Fig. 10C). Granules appeared similar to those observed in zone two. With wall dissolution and cell separation, granules filled intervening spaces and aggregated around immobilized bacteria.

Zone six. By 2 wk, hyperplastic cells farthest from the wound were bordered by smaller thick-walled cells with electron-dense opaque appositions on outer walls and at middle lamella corners. Intercellular spaces were filled with dense accumulations of osmophilic granules, fibers, and degenerating bacteria.

Epidermal rupture. Epidermal rupture occurred between 3 and 5 days after inoculation in the region of cell proliferation (Fig. 10D). Before rupture, bacteria were observed between adjacent epidermal cells and/or epidermal cells and cuticle. Cell wall and middle lamellar dissolution appeared similar to that observed in zones three and four. After rupture, host cells and high concentrations of intercellular bacteria extruded through the surface. Blister cells and nearby subsurface cells were often separated, hyperplastic, and thin-walled.

Secondary lesions. Epidermal ruptures often occurred over vascular tissue or oil glands. Although intracellular invasion of xylem vessels was occasionally observed, bacteria were not consistently observed within vascular or oil gland tissue and extensive cell division was not always present. Host cell walls and middle lamellae displayed similar degeneration patterns to those in primary lesions.

X. c. pruni. Bacteria occurred intercellularly in zones one and two and intracellularly in zone one but did not invade beyond wound barrier zones during the 2-wk sampling period. Organisms were observed as free intact dividing forms, free senescing forms, and degenerating forms within dense concentrations of osmophilic granules. Although many organisms were observed closely appressed to cell walls, attachment could not be definitely identified and bacteria appeared intact. Wound barrier zones were produced normally.

E. herbicola. Bacteria were present intercellularly in zones one and two and intracellularly in zone one. An immobilization reaction was observed at 24 hr in which organisms were surrounded by an intercellular fibrous and particulate matrix (Fig. 11A). Fibrous matrix components appeared similar to fibers lifting from nearby cell walls. After osmophilic granule induction, organisms were also observed degenerating within dense granular accumulations in zone two. At 2 wk, many bacteria were free of immobilizing substances with some intact and others degenerated.

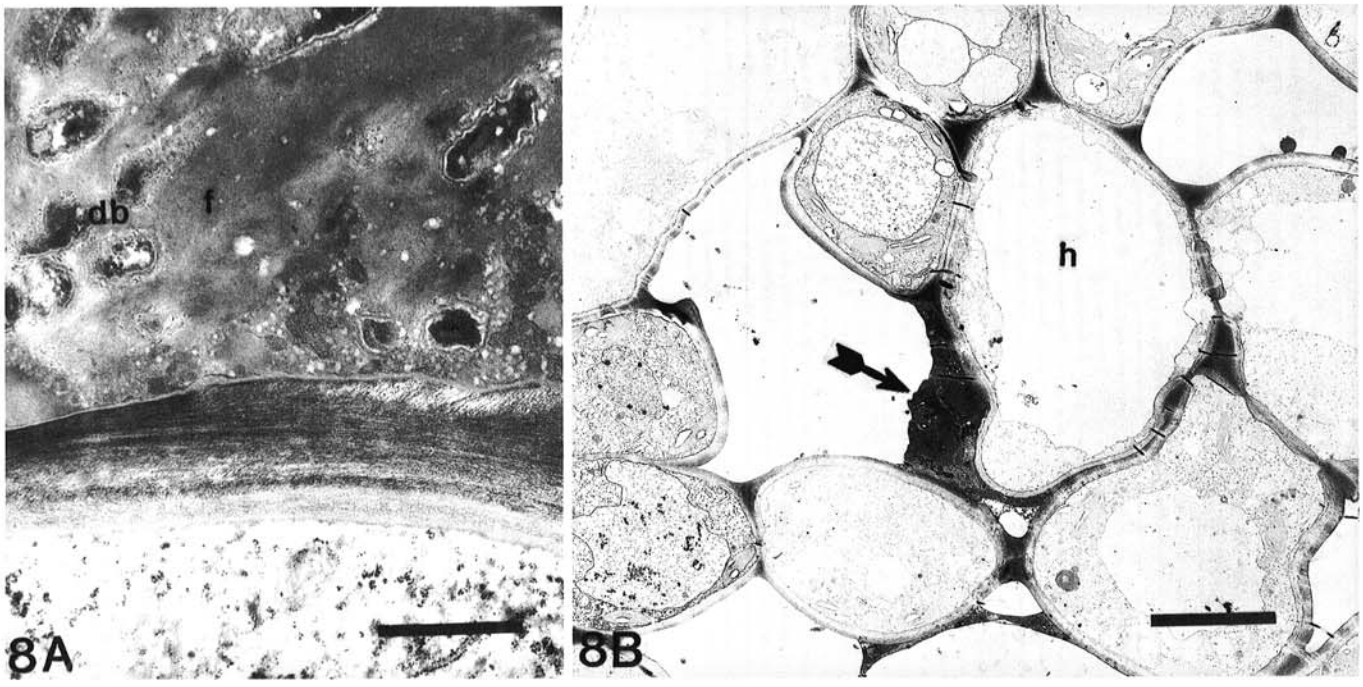

Fig. 8. Localization of strain F1 of *Xanthomonas campestris* pv. *citri* beyond wound repair zones in *Citrus aurantifolia*. **A,** Zone five, 7 days after inoculation. Degenerating bacteria (db) and increased electron density are present in the bacteria-associated fibrillar matrix (f). Bar = 1 μm. **B,** Immobilized bacteria (arrow) at the edge of invasion, zone five, bordered by zone six hypertrophic cells (h) similar to those indicating periderm development in healthy wound repair, 7 days after inoculation. Bar = 1 μm.

Wound barrier zones were produced normally, and organisms were not observed beyond zone three.

DISCUSSION

Wound repair. Foliar wound repair in *C. aurantifolia* culminates with the formation of a periderm and involves extensive ultrastructural modifications, many of which are associated with the cell wall. Most of these occur in zones two and three and are similar in appearance to those described elsewhere in impervious tissues and periderms formed during wound repair (1,4,5,6,8–12,22, 26–28,30). Protection against water loss and pathogenic entry afforded by impervious tissues and periderms has been attributed to such modifications. Surface lamellae and layered, cell wall thickening associated with wound repair of *C. aurantifolia* appear similar to descriptions of suberized and lignified cell walls. Although suberin may impregnate cell walls and extrude over outer cell wall surfaces (10–12), alternate depositions of lignin and

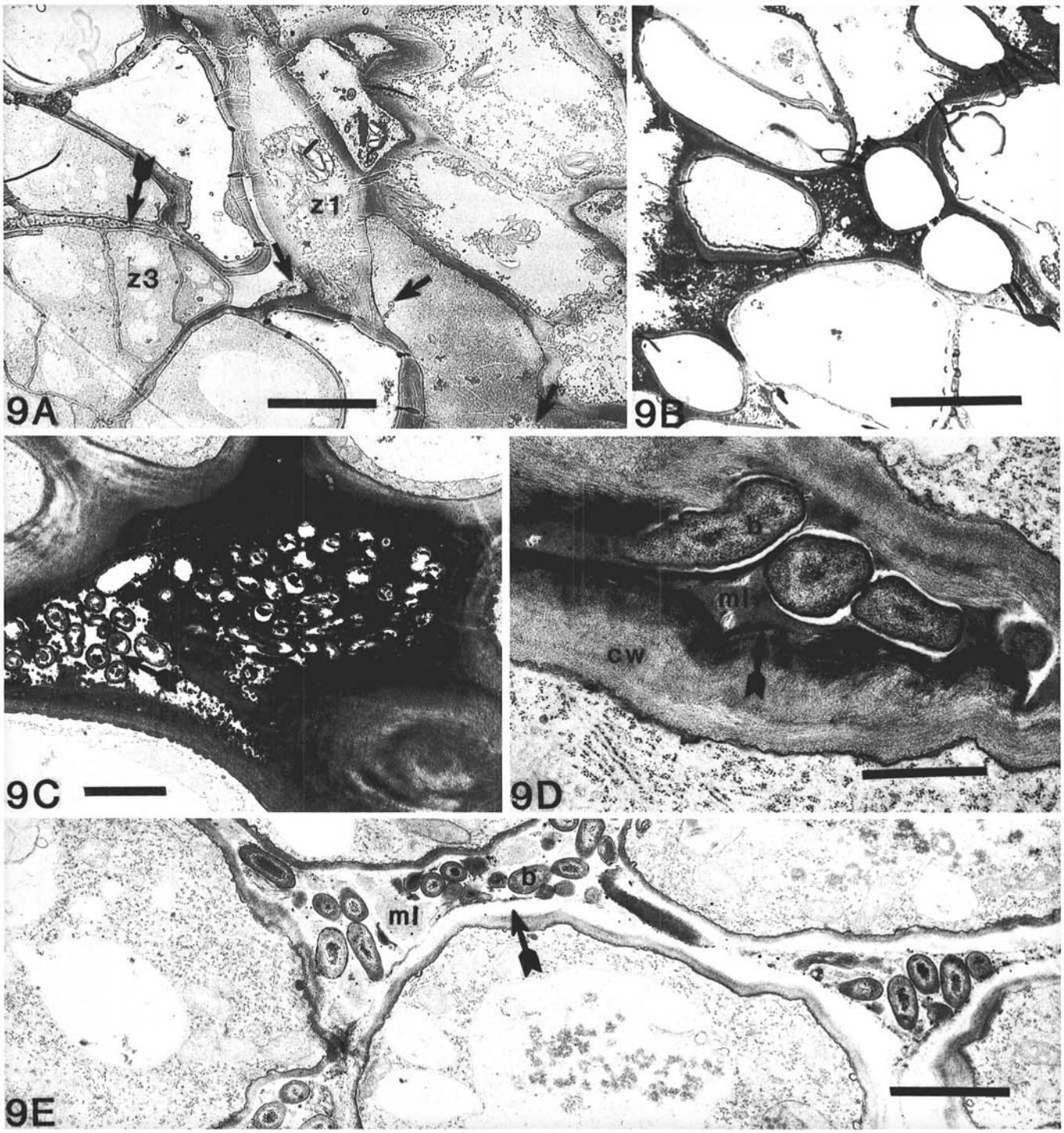

Fig. 9. Interactions between strain XC90 of *Xanthomonas campestris* pv. *citri* and wound repair in *Citrus aurantifolia*. **A,** Zones one (zl) and three (z3), 5 days after inoculation. Intact bacteria are entering zone three along middle lamella (arrow), and degenerating bacteria (arrowheads) appear in intercellular osmophilic granules. Zone two is absent. The wound is to the right. Bar = 10 μm. **B,** Remains of zone two and original cambium with dense accumulations of intercellular osmophilic substances, 2 wk after inoculation. The wound is to the left. Bar = 10 μm. **C,** High magnification of zone two osmophilic substances showing degenerating bacteria on the left (arrow) and complete bacterial immobilization on the right, 2 wk after inoculation. Bar = 2 μm. **D,** Early (4 days) bacterial (b) colonization of zone three middle lamella (ml), showing lifting of cell wall fibers (arrow). Bar = 1 μm. **E,** More advanced (5 days) bacterial (b) colonization of zone three middle lamella (ml), showing dissolution of middle lamella, and primary cell walls (arrow). Bar = 2.5 μm.

cellulose may cause a thick layered appearance (11). In addition to protecting against water loss, suberin and lignin physically exclude or sterically hinder bacterial enzymes that macerate pectin (12,23). Wax constituents in suberin/wax lamellae on inner walls also contribute to cell impermeability (6,10,28). Wall projections and granular appositions may have a role similar to pectic cell wall projections reported in carrot wound callus (9), which serve as middle lamellae when pressed between converging cell walls of developing periderms.

Amorphous intercellular deposits previously described in regions abutting wound periderms (1,8,9,11,12,26,27) have been associated with maintenance of water levels and protection against pathogens. These deposits have been variously identified as suberin (8,11,12,27), wound gums (1,11), pigments (26), and oils (9). In *C. aurantifolia*, extensive production of amorphous, wall-associated substances occurs during wound repair, but their composition is unknown. Osmophilic granules are the most abundant of these substances. Their heterogeneous properties of granule size, electron density, and tendency to aggregate suggest heterogeneity in chemical make-up and function. Among those functions, reinforcement of cell walls appears predominant. Granules may provide seals, congealing on outer wall surfaces to form surface lamellae or aggregating in more localized appositions over middle lamella corners. Their appearance in primary walls suggests that they contribute to internal wall thickening as well.

Host defense at the wound. Bacterial immobilization by granular, fibrous, or particulate substances released from cell walls forms the most prominent host defense, both at the wound and beyond. Some of these are similar to those produced normally during wound repair of uninoculated leaves. Bacterial

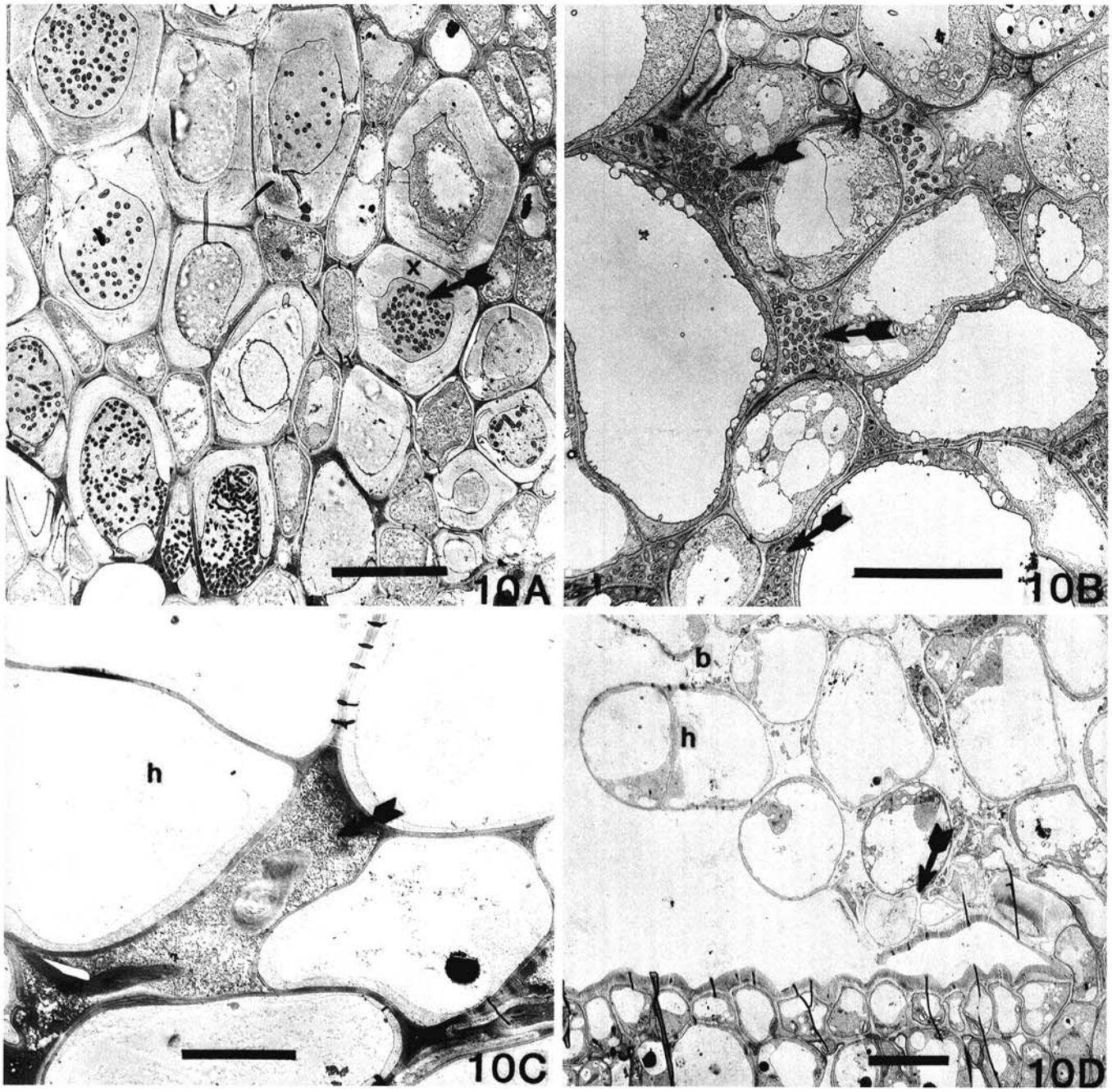

Fig. 10. Invasion and localization of strain XC90 of *Xanthomonas campestris* pv. *citri* beyond the wound in *Citrus aurantifolia*. **A,** Intracellular invasion (arrow) of xylem vessels (x), 14 days after inoculation. Bar = 10 μm. **B,** Bacterial invasion of middle lamella (arrows) between proliferating zone four cells, 14 days after inoculation. Bar = 10 μm. **C,** Edge of invasion showing osmophilic granules (arrow) in zone five bordered by hyperplasia (h), 2 wk after inoculation. Bar = 10 μm. **D,** Epidermal rupture showing degeneration of epidermal cell walls (arrow), thin-walled hyperplastic cells (h), and release of bacteria (b) from the host, 10 days after inoculation. Bar = 10 μm.

immobilization by cell wall granular and fibrous substances is well documented, although often not wound-related, and may be an induced (2,15,17,19,21), or passive reaction (18). Although mechanisms vary with host-bacterial combination, immobilization usually indicates a level of incompatibility between host and bacterium. In contrast, immobilization also occurs in the interactions between *C. aurantifolia* and the three pathogenic strains, which enter into compatible relationships. At the wound, osmophilic granules may serve as a broad spectrum defense mechanism, immobilizing organisms of each strain except for strain F1, which suppresses granule production. Although this appeared to be a passive response in strains F20, XP1, and EH1, strain XC90 may induce higher concentrations of granules as well as other osmophilic immobilizing substances. The immobilization of *E. herbicola* within 24 hr by substances within large patches of liberated cell wall fibers and a fibrous/particulate matrix represents a form of immobilization that is apparently associated with incompatibility.

Cell wall thickening at the wound also protects against bacterial damage, an effect observed most clearly in strain F20 infections in which phellem cell walls initially appear porous and degenerating but recover as granule concentrations increase. Cell wall thickening associated with lignification is reported to protect wounded citrus leaves from invasion by *X. c. citri* (22). Neither immobilization nor cell wall protection successfully restricts invasion of *X. c. citri* under the present conditions, probably because wound repair zones were not formed before inoculation.

Establishing infection involves more than circumventing wall thickening and immobilization mechanisms. Although *E. herbicola* and *X. c. pruni* were not completely immobilized at the wound, they failed to move beyond wound repair zones. Successful infection may involve numerous factors, including attachment of the pathogen or its extracellular polysaccharide to the host cell wall (29), the ability of extracellular polysaccharide to maintain a water-soaked state in the intercellular spaces, the presence of appropriate bacterial enzymes and toxins and the ability to overcome host antibacterial substances (3,14,19). Although intact dividing bacteria occurred in intercellular spaces, *E. herbicola* and *X. c. pruni* elicited significantly less effect on host cell walls than did strains of *X. c. citri*. Wall damage was minimal and interference with wound-induced wall modifications was absent, indicating that an inability to establish a successful relationship with the host cell wall may be one factor involved in incompatibility of the saprophyte and the non-citrus pathogen.

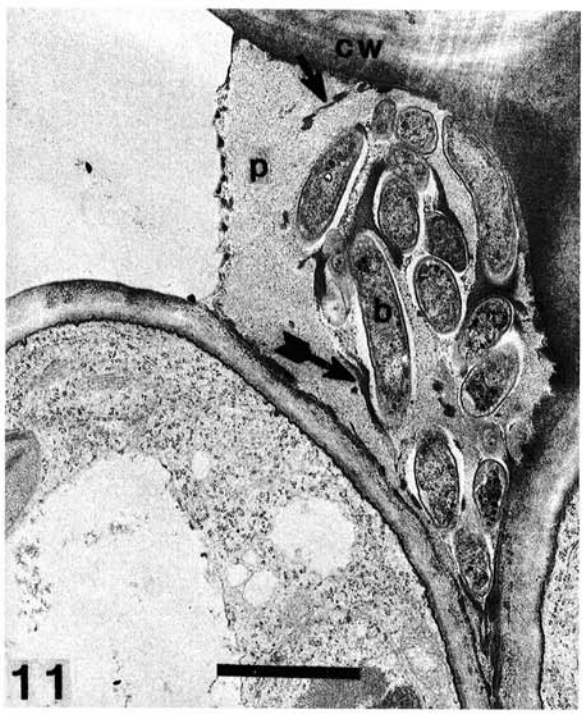

Fig. 11. Early (48 hr) immobilization of *Erwinia herbicola* in zone two intercellular space of wound-inoculated *Citrus aurantifolia*. Bacteria (b) are surrounded by particulate (p) material and fibers (arrow) similar to those (arrowhead) originating from host cell walls (cw). Bar = 2 m.

Localization beyond wound repair. Zone five bacterial immobilization in aggregating granules, cell wall protection by granule release, and zone six hypertrophy resemble wound defenses, with zones five and six corresponding to zones two and three, respectively. The possible dual nature of granule function at the wound, a function associated with wall thickening and bacterial immobilization, reappears in zone five of strain F20 infections. Granules are so densely compacted that organisms appear embedded in wall appositions. Suberization, lignification, and formation of impervious and meristimatic tissues are reported host responses to pathogenic invasion (1,4,5,13,20,25,26), supporting the conclusion that localization of *X. c. citri* is a modified wound response.

A similar localization pattern described for type A strains of *X. c. citri* was observed in resistant but not susceptible citrus varieties (20,21). Type A *X. c. citri* was immobilized in the intercellular spaces of resistant varieties by electron-dense materials originating from the host cell wall. While immobilizing substances were observed only in resistant varieties, both susceptible and resistant varieties developed meristematic tissue around lesion peripheries. The presence of the immobilization response in *C. aurantifolia* indicates that this mechanism of resistance can be present in susceptible varieties as well.

Strain differentiation. Differences in cytopathology among strains F20, F1, and XC90 are consistent with their different symptomatology. Blister formation in strain XC90 infections involves degradation of epidermal cell walls and cuticle separation followed by protrusion of proliferating host cells through epidermal ruptures. Strain F1 water-soaking may result from suppression of zone two and phellem modifications that leave internal tissues vulnerable to water loss through wounds. Because the ER has been identified as the source of suberin synthesis (23), it would be interesting to determine if an association exists between the prominent swollen ER and suberin suppression characteristic of F1 infections. Tonoplast and ER abnormalities displayed by host cells may indicate membrane damage with resulting cell leakage, which may add to fluids in intercellular spaces. In contrast, strain F20 infections, which do not induce water-soaking, also do not suppress wound repair or promote widespread host membrane damage.

Ultrastructure of each host-strain combination appeared distinctly different at each zone. Hence, strain F20 degraded cell walls without plasmalemma destruction in zone two, but with plasmalemma destruction and intracellular invasion in zones three and four. Strain F1 degraded middle lamellae only in atrophied periderm cells, appearing in intercellular spaces in zones four and five. Strain XC90 was not observed along middle lamellae until zone three developed. Changing interactions may result as host cell wall composition changes due to wound repair and the natural aging of the leaf. The presence of bacterial enzymes capable of degrading these different components may be strain dependent. Differences may also reflect different points of interference in the wound response, or concurrently, the host may display induced defense reactions dependent on the invading strain of bacteria. With the potential for host cell variability due to different experimental conditions, comparing ultrastructure with that reported elsewhere for other strains of *X. c. citri* is of limited value. Similarities, however, do exist between intracellular invasion by the Florida strains and that reported for a strain in the A group of *X. c. citri* (21).

The Florida strains appear to share several characteristics that differentiate them from strain XC90, including presence of fibrillar matrix, extensive colonization of intercellular spaces, limited affinity for middle lamellae, and failure to stimulate zone two granulation and zone three cell division. Such differences supplement the genomic fingerprinting, symptomatology, geographical distribution and host range differences presently used

to separate the type E Florida strains from type B strains of *X. c. citri* (7,16).

LITERATURE CITED

1. Akai, S., and Fukutomi, M. 1980. Performed internal physical defenses. Pages 139-159 in: Plant Disease, Vol. 5. J. G. Horsfall and E. B. Cowling, eds. Academic Press, New York. 534 pp.
2. Al-Mousawi, A. H., Richardson, P. E., Essenberg, M., and Johnson, W. M. 1983. Specificity of the envelopment of bacteria and other particles in cotton cotyledons. Phytopathology 73:484-489.
3. Anderson, A. J. 1982. Preformed resistance mechanisms. Pages 119-136 in: Phytopathogenic Prokaryotes, Vol. 2. M. S. Mount and G. H. Lacy, eds. Academic Press, New York. 506 pp.
4. Biggs, A. R. 1984. Boundary-zone formation in peach bark in response to wounds and *Cytospora leucostoma* infection. Can. J. Bot. 62:2814-2821.
5. Biggs, A. R., Davis, D. D., and Merrill, W. 1983. Histopathology of cankers on *Populus* caused by *Cytospora chrysosperma*. Can. J. Bot. 61:563-574.
6. Biggs, A. R., and Stobbs, L. W. 1986. Fine structure of the suberized cell walls in the boundary zone and necrophylactic periderm in wounded peach bark. Can. J. Bot. 64:1606-1610.
7. Civerolo, E. L. 1984. Bacterial canker disease of citrus. J. Rio Grande Vall. Hortic. Soc. 37:127-146.
8. Cline, M. N., and Neely, D. 1983. The histology and histochemistry of the wound healing process in geranium cuttings. J. Am. Soc. Hortic. Sci. 108:496-502.
9. Davies, W. P., and Lewis, B. G. 1981. Development of pectic projections on the surface of wound callus cells of *Daucus carota* L. Ann. Bot. 47:409-413.
10. Dean, B. B., Kolattukudy, P. E., and Davis, R. W. 1977. Chemical composition and ultrastructure of suberin from hollow heart tissue of potato tubers (*Solanum tuberosum*). Plant Physiol. 59:1008-1010.
11. Esau, K. 1965. Plant Anatomy. Second ed. John Wiley & Sons, New York. 767 pp.
12. Fox, R. T. V., Manners, J. G., and Myers, A. 1971. Ultrastructure of entry and spread of *Erwinia carotovora* var. *atroseptica* into potato tubers. Potato Res. 14:61-73.
13. Goodman, R. N. 1980. Defenses triggered by previous invaders: Bacteria. Pages 305-316 in: Plant Disease, Vol. 5. J. G. Horsfall and E. B. Cowling, eds. Academic Press, New York. 535 pp.
14. Goodman, R. N. 1982. The infection process. Pages 31-62 in: Phytopathogenic Prokaryotes, Vol. 1. M. S. Mount and G. H. Lacy, eds. Academic Press, New York. 541 pp.
15. Goodman, R. N., Huang, P. Y., and White, J. A. 1976. Ultrastructural evidence for immobilization of an incompatible bacterium, *Pseudomonas pisi*, in tobacco leaf tissue. Phytopathology 66:754-764.
16. Hartung, J. S., and Civerolo, E. L. 1987. Genomic fingerprints of *Xanthomonas campestris* pv. *citri* strains from Asia, South America, and Florida. Phytopathology 77:282-285.
17. Huang, P. Y., Huang, J. S., and Goodman, R. N. 1975. Resistance mechanisms of apple shoots to an avirulent strain of *Erwinia amylovora*. Physiol. Plant Pathol. 6:283-287.
18. Jones, S. B., and Fett, W. F. 1985. Fate of *Xanthomonas campestris* infiltrated into soybean leaves: An ultrastructural study. Phytopathology 75:733-741.
19. Keen, N. T., and Holliday, M. J. 1982. Recognition of bacterial pathogens by plants. Pages 179-217 in: Phytopathogenic Prokaryotes, Vol. 2. M. S. Mount and G. H. Lacy, eds. Academic Press, New York. 506 pp.
20. Koizumi, M. 1977. Behavior of *Xanthomonas citri* (Hasse) Dowson and histological changes of diseased tissues in the process of lesion extension. Ann. Phytopathol. Soc. Jpn. 43:129-136.
21. Koizumi, M. 1979. Ultrastructural changes in susceptible and resistant plants of citrus following artificial inoculation with *Xanthomonas citri* (Hasse) Dowson. Ann. Phytopathol. Soc. Jpn. 45:635-644.
22. Koizumi, M. 1983. Relationship between wound-healing process of citrus leaf tissues and successful infection through wounds by *Xanthomonas campestris* pv. *citri* (Hasse) Dye. Ann. Phytopathol. Soc. Jpn. 49:352-360.
23. Kolattukudy, P. E., and Dean, B. B. 1974. Structure, gas chromatographic measurement, and function of suberin synthesized by potato tuber tissue slices. Plant Physiol. 54:116-121.
24. Lawson, R. H., Dienelt, M. M., and Civerolo, E. L. 1989. Histopathology of *Xanthomonas campestris* pv. *citri* from Florida and Mexico in wound-inoculated detached leaves of *Citris aurantifolia*: Light and scanning electron microscopy. Phytopathology 79:329-335.
25. Maule, A. J., and Ride, J. P. 1982. Ultrastructure and autoradiography of lignifying cells in wheat leaves wound-inoculated with *Botrytis cinerea*. Physiol. Plant Pathol. 20:235-241.
26. Mullick, D. B. 1977. The non-specific nature of defense in bark and wood during wounding, insect and pathogen attack. Pages 395-441 in: Recent Advances in Phytochemistry 11. F. A. Loewus and V. C. Runeckles, eds. Plenum Press, New York. 527 pp.
27. Rittinger, P. A., Biggs, A. R., and Peirson, D. R. 1987. Histochemistry of lignin and suberin deposition in boundary layers formed after wounding in various plant species and organs. Can. J. Bot. 65:1886-1892.
28. Soliday, C. L., Kolattukudy, P. E., and Davis, R. W. 1979. Chemical and ultrastructural evidence that waxes associated with the suberin polymer constitute the major diffusion barrier to water vapor in potato tuber (*Solanum tuberosum* L.). Planta 146:607-614.
29. Takahashi, T., and Doke, N. 1985. Purification and partial characterization of an agglutinin in citrus leaves against extracellular polysaccharides of *Xanthomonas campestris* pv. *citri*. Physiol. Plant Pathol. 27:1-13.
30. Wood, R. K. S. 1960. Chemical ability to breach the host barriers. Pages 233-272 in: Plant Pathology: An Advanced Treatise. II. J. G. Horsfall and A. E. Dimond, eds. Academic Press, New York. 715 pp.